



Review

Direct Laser Interference Patterning of Bioceramics: A Short Review

Douglas Fabris ¹, Andrés Fabián Lasagni ^{2,3}, Márcio C. Fredel ¹ and Bruno Henriques ^{1,4,*}

¹ Campus Trindade, Ceramic and Composite Materials Research Group (CERMAT), Federal University of Santa Catarina (UFSC), 88040-900 Florianópolis/SC, Brazil; douglas.df1@gmail.com (D.F.); m.fredel@ufsc.br (M.C.F.)

² Institute for Manufacturing Technology, Technische Universität Dresden, 01062 Dresden, Germany; andres_fabian.lasagni@tu-dresden.de

³ Fraunhofer IWS, Winterbergstr. 28, 01277 Dresden, Germany

⁴ Campus de Azurém, CMEMS-UMinho, University of Minho, 4800-058 Guimarães, Portugal

* Correspondence: brunohenriques@dem.uminho.pt

Received: 6 August 2019; Accepted: 11 October 2019; Published: 28 October 2019



Abstract: Bioceramics are a great alternative to use in implants due to their excellent biocompatibility and good mechanical properties. Depending on their composition, bioceramics can be classified into bioinert and bioactive, which relate to their interaction with the surrounding living tissue. Surface morphology also has great influence on the implant biological behavior. Controlled texturing can improve osseointegration and reduce biofilm formation. Among the techniques to produce nano- and micropatterns, laser texturing has shown promising results due to its excellent accuracy and reproducibility. In this work, the use of laser techniques to improve surface morphology of biomaterials is reviewed, focusing on the application of direct laser interference patterning (DLIP) technique in bioceramics.

Keywords: laser; direct laser interference patterning; texturing; bioceramics

1. Introduction

Bioceramics have been studied for biomedical applications due to their excellent biocompatibility and low wear rates. Alumina, for example, presents high mechanical resistance, adequate fracture toughness and great resistance to wear and corrosion. However, a high failure rate of alumina implants has been reported due to slow crack growth during *in vivo* studies [1]. Zirconia, on the other hand, has presented excellent mechanical properties and biocompatibility, even better than alumina, being used mainly in dental implants and as ball heads for total hip replacement surgery [2]. Furthermore, in dental implants, zirconia has been introduced as an alternative to the conventional titanium implants due to its better aesthetic. In addition, it has demonstrated low bacteria colonization and good biocompatibility, providing favorable soft-tissue integration [3].

Zirconia and alumina are bioinert materials, i.e., they do not interact with biological tissues creating no direct bone–implant interface. In fact, inert implants are isolated from the surrounding tissues by a collagenous capsule which is formed after the implantation [4]. Thus, the implant stability relies mainly on the mechanical interlocking with the bone. On the other hand, bioactive materials, such as hydroxyapatite (HA), tricalcium phosphate (TCP) and bioactive glasses (Bioglass), can be osteoconductive and osteoinductive, providing suitable surfaces for osteoblasts adhesion and proliferation, bonding to soft and/or hard tissue [5]. However, despite their excellent biocompatibility, bioactive materials are very brittle, being used only as coating or in small bone grafts (scaffolds). In scaffolds, to achieve the osteoconductive capability, besides their bioactivity,

the structure must have hierarchical and interconnected porosity of over 90% to allow for bone ingrowth. Macropores (diameter $>50\ \mu\text{m}$) and micropores (diameter $<20\ \mu\text{m}$) play important roles in cell colonization and vascularization and in interactions between cells and matrix, respectively [6].

In addition to material composition, surface topography of implants has a great influence on their biological behavior and, consequently, on their performance, even on bioinert ceramics. Studies have shown that increasing roughness of the implant surface can improve primary and long-term stabilization due to an anchorage effect on the bone [7]. Surfaces with controlled roughness can also lead to higher cell proliferation and improved protein synthesis compared to a flat surface [8]. This effect can be noticed on bioactive ceramics as well. Nano-scale features can improve biological properties of bioactive glass, such as enhanced apatite formation and cell attachment and proliferation [9]. Micro/nano-topographies on bioactive coatings can also improve adhesion of cells to the implant [10]. There are several methods to increase surface roughness of implants, such as plasma spray, grit-blasting, acid etching and anodizing [11]. However, these techniques are characterized for producing only random surface patterns. Multi-scale and controlled pattern orientation and size can improve osseointegration by mimicking the cells natural environment [12,13]. While microtopography (features size of $<50\ \mu\text{m}$) aims to create structures with cellular, subcellular and macromolecular scale enhancing osseointegration, nanotopography (features size of $<500\ \text{nm}$) covers the molecular and atomic scale, facilitating cell adhesion and mineral nucleation [14]. A combination of micro- and nano-scale features in implants seems to enhance bone regeneration [15,16]. The surface pattern direction also influences the cell growth orientation [17]. In this context, laser treatments can provide a better control of the micro- and nano-topography of the implant surface and enhance osseointegration [18].

Besides biocompatibility, microbial infection is another main factor directly related to the implant success. Bacterial colonization and biofilm formation can occur during surgery, due to implant poor handling and environment control, or after surgery [19]. For example, adsorption of salivary pellicle during the healing stage of dental implants induces bacterial accumulation [20]. This infection can lead to destruction of the adjacent tissue or even implant failure [21]. Several techniques have been developed to decrease bacterial adherence and proliferation on implant surface. These techniques include chemical modification, such as coating with antibacterial agents, and physical modification of the surface morphology [22,23]. However, chemical modifications can present possible drawbacks, such as toxicity, reduced efficiency over time and natural selection of bacteria resistant to the chemical agent. On the other hand, studies have shown the influence of surface topography of implants on adhesion and proliferation of bacteria. While random surface pattern (microroughness) can increase bacteria proliferation [24], controlled textured surfaces can reduce the bacteria adhesion and biofilm formation [25]. Additionally, in this application field, laser surface texturing has shown to be capable of reducing significantly bacterial adhesion and biofilm formation when producing textured surfaces, being a promising method to decrease the risk of infection of implants [25].

Most conventional machining techniques can fabricate only patterns with a minimum size of around $100\ \mu\text{m}$ in ceramics. Fabrication of patterns smaller than that can be very challenging due to their hardness and low fracture toughness. Therefore, conventional techniques cannot achieve proper surface topology to improve osseointegration or decrease microbial adhesion of implants. In this context, laser treatment processes offer a fast and accurate patterning method able to produce micro- and nano-scale patterns in ceramic surfaces. Especially, laser patterning with direct laser interference patterning (DLIP) is a promising technique that permits the fabrication of periodic arrays in a great range of materials (metals, polymers and ceramics) in a single-step process [26].

2. Laser Modifications of Bioceramics

As stated before, surface characteristics of biomaterials have great influence on their performance during *in vivo* use. Controlled surface topography can improve osseointegration and reduce bacterial adhesion to orthopedic and dental implants. However, controlled nano- and micro-textures cannot be easily achieved using conventional methods, especially in bioceramics, which are hard and brittle

and consequently difficult to process. Zirconia, for example, can undergo microstructural changes due to high stresses developed during conventional machining. Laser processing has shown to be a promising alternative to fabrication of surface textures in bioceramics based on photothermal and photochemical ablation mechanisms, and thus allowing inducing locally controlled changes in the implants surfaces. However, these thermal loads can also affect the ceramics microstructure as well as the surface chemistry. The high thermal loads caused by laser–material interaction can induce transformation toughening on the zirconia surface [27]. HA can also have its chemical structure modified by the laser treatment. Loss of crystallinity and transformation of HA into other phosphates have been reported in the literature, which can change its biological properties [28]. On the other hand, chemical modification of HA due to laser treatment can produce multiphase structure and improve osteoconductivity of biomaterials [29]. Reports indicate that alumina can also present problems during laser surface processing, such as cracking and microstructure changes [30,31]. These problems can prevail over the benefits of the surface texture, and thus the influence of the laser treatment conditions on these material characteristics has to be carefully evaluated. There are several laser parameters, such as wavelength, energy density of laser beam, mode of operation (continuous or pulsed) and pulse duration, which can change the material removal phenomena occurring at its surface. For ablation of ceramics, high-intensity pulsed lasers are preferred as the processing parameters are more effectively controlled compared to those of lasers in continuous mode [32].

Conventional machining of ceramics can be a challenge due to their high hardness and low fracture toughness, resulting in high tool wear, low material removal rates, and mechanical and thermal damage to the piece. In this context, laser machining can be an alternative to these methods. In this process, a high-density laser beam is incident on the work piece and the material is removed by melting, dissociation, evaporation and expulsion from the area of laser–material interaction [32]. Samant and Dahotre used a pulsed Nd:YAG laser (wavelength: 1064 nm) to machine cavities on structural ceramics (Al_2O_3 , Si_3N_4 , SiC and MgO) successfully [33]. Yang et al. machined alumina green bodies produced via gelcasting using a CO_2 laser (wavelength: 10.6 μm), showing that ceramic bodies with complex shapes can be fabricated using laser machining [34]. Li et al. machined zirconia (Y-TZP) bodies using a solid-state nanosecond laser (wavelength: 532 nm), producing high-quality micro-sized steps and blind holes. It is important to state that no phase modification of zirconia was observed after laser machining in this study [35]. In another study, alumina/zirconia (75/25 wt%) composites in the format of discs and acetabular cups were also successfully machined using laser ablation, creating a surface roughness that could be modulated from 3 to 30 μm , in highly arranged or random textures [36]. Laser ablation can also improve adhesion of zirconia to other materials, such as dental veneering porcelain, creating a mechanical interlocking effect due to the holes machined on the zirconia surface [37]. Several other studies show the feasibility of laser surface treatment in alumina and zirconia, which can improve significantly their biological performance [38].

Berger et al. used a Nd:YAG laser operating at a wavelength of 355 nm (in a UV region) with a microlens array (MLA), which produces multiple foci from a single laser beam, to fabricate alumina-, zirconia- and HA-patterned surfaces [39]. In their results, all three materials were successfully patterned using this method. HA samples presented the largest dimples depth, which can be explained by its lowest temperature of decomposition and fusion, while the smallest dimples structures were observed at the alumina samples, probably due to its highest thermal conductivity.

Holthaus et al. compared several micropatterning methods (microtransfer molding, modified micromolding, Aerosol-Jet[®] printing, CNC-micromachining, traditional laser ablation and DLIP) in ceramic surfaces (zirconia, alumina, silica and HA). Using laser ablation with a Nd:YAG laser (wavelength: 1064 nm), they achieved relatively good patterning results, although ablated pattern edges looked inaccurate and the pattern surface had higher roughness than those obtained with the other techniques. In the DLIP technique, the same Nd:YAG laser was used, but a wavelength of 266 nm was obtained using a harmonic generation method. This technique showed better accuracy on pattern edges and much lower roughness compared to the conventional laser ablation, since the absorption

efficiency of the laser radiation was increased at a shorter wavelength, as well as the probability of producing surface textures by photochemical ablation mechanism. This is also a very fast patterning process of large areas compared to the other studied methods [40].

3. Direct Laser Interference Patterning

Differently from conventional direct laser writing, in DLIP, a laser beam is split into two or more beams which are subsequently superposed at the material' surface. In this way, an interference pattern is created, and its direct application on materials results in well-defined surface textures. For instance, using a two-beam configuration (see Figure 1a), a line-like periodic variation of the laser energy is obtained (Figure 1b) and the lateral dimension of the periodic pattern (spatial period P) can be controlled by the intercepting angle between the individual sub-beams, as described in Equation (1) [41]:

$$P = \lambda/2\sin(\theta), \quad (1)$$

where λ and θ denote the laser wavelength and half-angle between interfering beams, respectively.

By controlling also the number of beams, beam intensities and polarization, it is also possible to produce other pattern geometries such as dot-like, pillar-like and lamella-like structures. DLIP allows for a high-speed single-step surface patterning process in a wide range of materials, including polymers, metal and ceramics. The main advantage of DLIP over other laser techniques is that the pattern is engraved over the exposed surface at the same time, instead of being created by the conventional laser scanning over the geometry [42]. Further details about this technique can be found in [43].

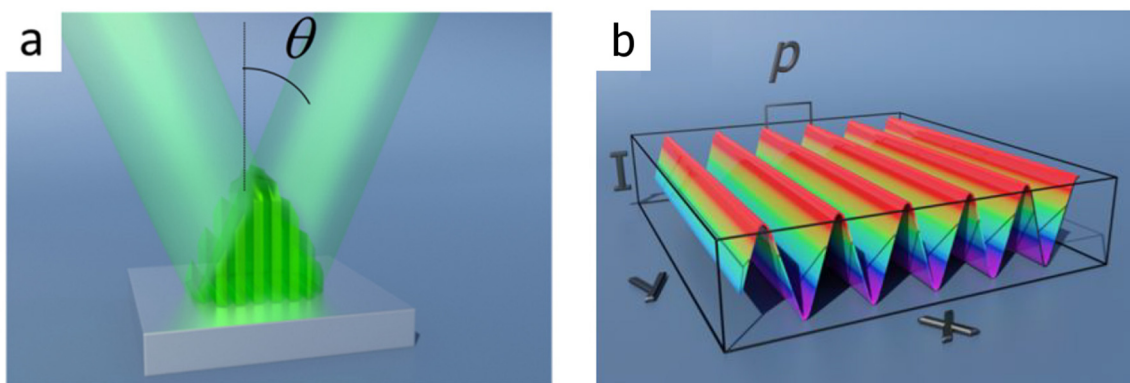


Figure 1. Two beams interference system (a) and the calculated intensity distribution (b), which create the pattern. Different numbers of beams create different patterns. Adapted from [44].

For biomaterials, selective ablation at the interference maxima creates micropatterns that increase surface roughness and can guide cell growth in a specific direction. Unlike some other surface modification techniques, DLIP allows for an efficient control of periodic array dimensions controlling the laser processing parameters [41]. DLIP has been widely researched in biomedical applications, mainly in polymers and metals.

Guenther et al. used DLIP on polymeric materials (polyimide and polystyrene) to show the influence of the material topography on the bacteria adhesion behavior under in vivo and in vitro conditions. The results showed that 1-D line-like structures can increase bacteria adherence. On the other hand, complex 3-D patterns (lamella-like) prevented biofilm formation [45]. Similar results were achieved by Valle et al., who showed that pillar and line topographies produced via DLIP increase bacteria adhesion to polymers compared to non-patterned samples, while more irregular and complex lamellar topography reduced adhesion [46]. Furthermore, Langheinrich et al. studied cell growth behavior over polyimide patterned with substrates using DLIP to fabricate line-like arrays, showing that the cells aligned to the pattern direction, i.e., they sensed and responded to the change

of topology induced by the laser patterning. Thus, they concluded that DLIP is a suitable method to control cell growth for medical and biological applications [47].

DLIP can be also used to improve the osseointegration of implants and, consequently, its performance. Zwahr et al. showed that DLIP increases cell viability on titanium surface compared to traditional surface treatments such as acid etching and grit blasting. This result can be explained by an enhanced metabolism of cells on the laser-treated surface and it could improve healing processes and long-term stability of implants [48].

DLIP has been also successfully applied in zirconia substrates without undesirable changes in microstructure and it can even increase its mechanical resistance [49,50]. However, proper control of laser parameters is necessary to achieve surface textures with high feature quality. For example, increasing the number of pulses and the laser energy density can increase depth of patterned structures; however, it has a detrimental effect on surface finishing due to formation of porosity [51]. DLIP can also generate a steep thermal gradient on the surface, which can cause microcracking, directional recrystallization and phase transformation [42,52]. Thus, it is important to optimize laser parameters to achieve the desirable surface patterns with good quality. Figure 2 shows both the surface and cross-sectional images of zirconia textured using DLIP with wavelengths of 532 nm and 355 nm. The authors employed different optical setup line-like patterns with different periodicities (4, 10 and 15 μm) to texture the surface. However, intergranular cracks homogeneously distributed all over the surface with a maximum depth of 1 μm were observed for all wavelengths and periodicities tested. Furthermore, the laser treatment caused recrystallization, with formation of elongated grains perpendicular to the surface and phase transformation from tetragonal to monoclinic mainly around the crack network [42].

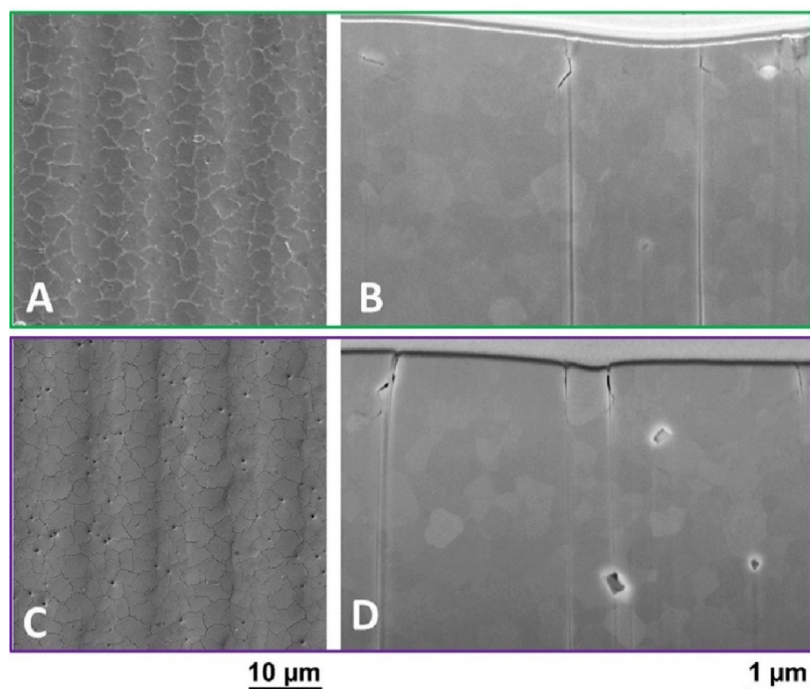


Figure 2. Surface and cross-sectional images of zirconia patterned with direct laser interference patterning (DLIP) for two wavelengths: 532 nm (A,B) and 355 nm (C,D). Adapted from [42].

DLIP also has been used in hydroxyapatite (HA) substrates to fabricate surface to improve biocompatibility. Berger et al. used a Nd:YAG laser operating at wavelengths of 266 nm and 355 nm to produce line- and cross-like patterns with different numbers of pulses and beam energy densities. In their study, they also observed that the pattern depth increased with the pulse number, but its quality decreased with higher energies. The best results were achieved using a low–medium energy density

and a moderate number of pulses. In addition, the laser with a wavelength of 266 nm presented better resolution for smaller patterns due to a higher photochemical contribution to the ablation process. The line-like patterns were achieved by using a periodicity of 20 μm , a wavelength of 355 nm, 10 pulses and a fluence of 1.2 J/cm^2 (Figure 3a) and by using a periodicity of 10 μm , a wavelength of 266 nm, 10 pulses and a fluence of 0.6 J/cm^2 (Figure 3b). Better resolution by using the wavelength of 266 nm can be noted, as well as the need of lower fluence to achieve the desired patterning [53].

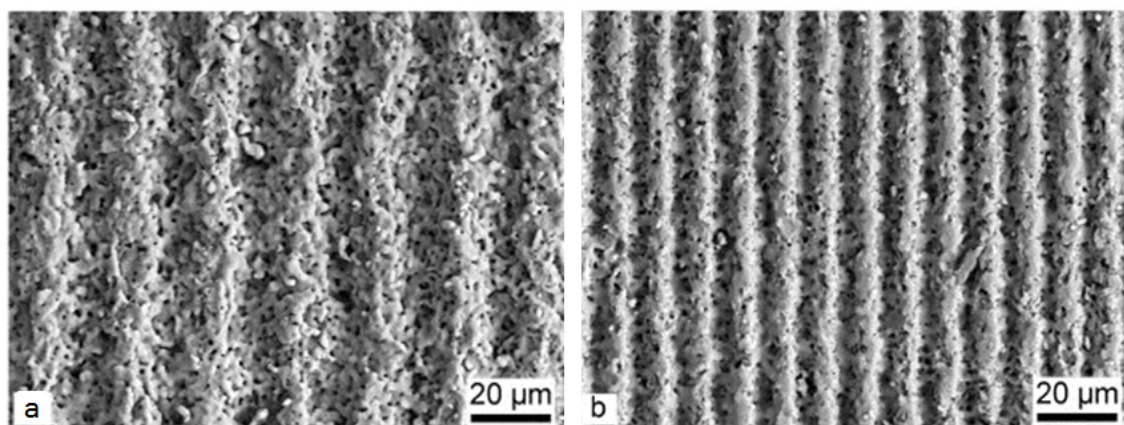


Figure 3. (a) Line-like patterns on hydroxyapatite produced with DLIP using a laser wavelength of 355 nm and a periodicity of 20 μm ; and (b) line-like patterns on hydroxyapatite produced with DLIP using a laser wavelength of 266 nm and a periodicity of 10 μm . Adapted from [53].

In addition to HA, alumina was also successfully patterned using DLIP [50]. This study showed that the laser treatment can even improve flexural strength of dental ceramics (alumina and zirconia). This effect can be explained by the formation of a periodic distribution of pores sizes and grain refinement. However, to the best of our knowledge, only studies regarding the influence of DLIP-patterned textures in bioceramics on their biological properties, such as osseointegration and biofilm formation, have been conducted until now. An overview of the already performed studies related with the application of DLIP in bioceramics is shown in Table 1. Studies on this topic are still scarce, but these works show the feasibility of bioceramics laser processing with different parameters.

Table 1. Studies using DLIP on bioceramics in the literature.

| Authors | Material | Laser Information |
|---------------------|-------------------|--|
| Daniel et al. [49] | 8% Ytria FSZ | Nd:YAG, wavelength: 355 nm, pulse duration: 2.5 ns, pulse number: 1 to 100 pulses applied, fluence: 0.2–0.9 J/cm^2 |
| Daniel et al. [50] | Y-PSZ and Alumina | Nd:YAG, wavelength: 355 nm, pulse duration: 2.5 ns, pulse number: 1, 10 and 50 pulses applied, fluence: 0.35–0.95 J/cm^2 |
| Roitero et al. [51] | 3Y-TZP | Nd:YAG, wavelength: 355 nm, pulse duration: 10 ns, pulse number: 1–10 pulses applied, fluence: 0.15–7.15 J/cm^2 |
| Roitero et al. [42] | 3Y-TZP | Nd:YAG, wavelength: 355 and 532 nm, pulse duration: 10 ns, pulse number: single pulse applied, fluence: 3.5 and 4 J/cm^2 |
| Roitero et al. [52] | 3Y-TZP | Nd:YAG, wavelength: 532 nm, pulse duration: 10 ns, pulse number: single pulse applied, fluence: 4 J/cm^2 |
| Berger et al. [53] | Hydroxyapatite | Nd:YAG, wavelength: 266 and 355 nm, pulse duration: 10 ns, pulse number: 1–100 pulses applied, fluence: 0.6–2.4 J/cm^2 |

4. Conclusions

Laser processing has been emerging as a powerful technique to produce surface modifications on hard and/or brittle bioceramic materials such as zirconia, alumina and calcium phosphates. Despite the advances seen so far on the ability to produce nano- and micro-biofunctional structures at high

throughputs as demonstrated by the DLIP technique, there are still several limitations that need to be overcome. The major challenges remain on avoiding the problems caused by the low thermal shock resistance of these materials that cause undesired nano- and/or micro-cracks. At the same time, promising results have been reported on the ability to enhance the flexural strength and biological response of these materials using the same techniques. Novel developments on materials properties and design, laser equipment and/or processing strategies are thus expected in order to make the most of the laser processing technology applied to bioceramics.

Author Contributions: The contribution of the authors to this paper was as follows: Conceptualization, B.H.; methodology, B.H. and D.F.; investigation, D.F.; writing of original draft preparation, D.F., B.H., M.C.F. and A.F.L.; writing of review and editing, M.C.F. and A.F.L.

Funding: This study was funded by FCT-Portugal through the following projects—UID/EEA/04436/2013, COMPETE 2020 with the code POCI-01-0145-FEDER-00694 and LaserMULTICER (POCI-01-0145-FEDER-031035) and by Conselho Nacional de Desenvolvimento Científico e Tecnológico (CNPq), Brazil through the project—CNPq/UNIVERSAL/421229/2018-7. B.H. acknowledges the support of the Alexander von Humboldt Foundation.

Conflicts of Interest: The authors declare no conflict of interest. The funders had no role in the design of the study; in the collection, analyses, or interpretation of data; in the writing of the manuscript, or in the decision to publish the results.

References

1. De Aza, A.H.; Chevalier, J.; Fantozzi, G.; Schehl, M.; Torrecillas, R. Crack growth resistance of alumina, zirconia and zirconia toughened alumina ceramics for joint prostheses. *Biomaterials* **2002**, *23*, 937–945. [[CrossRef](#)]
2. Sennerby, L.; Dasmah, A.; Larsson, B.; Iverhed, M. Bone Tissue Responses to Surface-Modified Zirconia Implants: A Histomorphometric and Removal Torque Study in the Rabbit. *Clin. Implant Dent. Relat. Res.* **2006**, *7*, 13–20. [[CrossRef](#)]
3. Nascimento, C.D.; Pita, M.S.; Fernandes, F.H.N.C.; Pedrazzi, V.; de Albuquerque Junior, R.F.; Ribeiro, R.F. Bacterial adhesion on the titanium and zirconia abutment surfaces. *Clin. Oral Implants Res.* **2014**, *25*, 337–343. [[CrossRef](#)] [[PubMed](#)]
4. Castner, D.G.; Ratner, B.D. Biomedical surface science: Foundations to frontiers. *Surf. Sci.* **2002**, *500*, 28–60. [[CrossRef](#)]
5. Salinas, A.J.; Vallet-Regí, M. Bioactive ceramics: From bone grafts to tissue engineering. *RSC Adv.* **2013**, *3*, 11116. [[CrossRef](#)]
6. Karageorgiou, V.; Kaplan, D. Porosity of 3D biomaterial scaffolds and osteogenesis. *Biomaterials* **2005**, *26*, 5474–5491. [[CrossRef](#)] [[PubMed](#)]
7. Buser, D.; Schenk, R.K.; Steinemann, S.; Fiorellini, J.P.; Fox, C.H.; Stich, H. Influence of surface characteristics on bone integration of titanium implants. A histomorphometric study in miniature pigs. *J. Biomed. Mater. Res.* **1991**, *25*, 889–902. [[CrossRef](#)]
8. Groessner-Schreiber, B.; Tuanf, R.S. Enhanced extracellular matrix production and mineralization by osteoblasts cultured on titanium surfaces in vitro. *J. Cell Sci.* **1992**, *101*, 209–217.
9. Lei, B.; Chen, X.; Wang, Y.; Zhao, N.; Du, C.; Fang, L. Surface nanoscale patterning of bioactive glass to support cellular growth and differentiation. *J. Biomed. Mater. Res. Part A* **2010**, *94*, 1091–1099. [[CrossRef](#)]
10. Zhang, W.; Wang, G.; Liu, Y.; Zhao, X.; Zou, D.; Zhu, C.; Jin, Y.; Huang, Q.; Sun, J.; Liu, X.; et al. The synergistic effect of hierarchical micro/nano-topography and bioactive ions for enhanced osseointegration. *Biomaterials* **2013**, *34*, 3184–3195. [[CrossRef](#)]
11. Le Guéhennec, L.; Soueidan, A.; Layrolle, P.; Amouriq, Y. Surface treatments of titanium dental implants for rapid osseointegration. *Dent. Mater.* **2007**, *23*, 844–854. [[CrossRef](#)]
12. Lim, J.Y.; Donahue, H.J. Cell Sensing and Response to Micro- and Nanostructured Surfaces Produced by Chemical and Topographic Patterning. *Tissue Eng.* **2007**, *13*, 1879–1891. [[CrossRef](#)] [[PubMed](#)]
13. Dumas, V.; Rattner, A.; Vico, L.; Audouard, E.; Dumas, J.C.; Naisson, P.; Bertrand, P. Multiscale grooved titanium processed with femtosecond laser influences mesenchymal stem cell morphology, adhesion, and matrix organization. *J. Biomed. Mater. Res. Part A* **2012**, *100*, 3108–3116. [[CrossRef](#)] [[PubMed](#)]

14. Fernandez-Yague, M.A.; Abbah, S.A.; McNamara, L.; Zeugolis, D.I.; Pandit, A.; Biggs, M.J. Biomimetic approaches in bone tissue engineering: Integrating biological and physicochemical strategies. *Adv. Drug Deliv. Rev.* **2015**, *84*, 1–29. [[CrossRef](#)] [[PubMed](#)]
15. Günther, D.; Scharnweber, D.; Hess, R.; Wolf-Brandstetter, C.; Holthaus, M.G.; Lasagni, A.F. High precision patterning of biomaterials using the direct laser interference patterning technology. In *Laser Surface Modification of Biomaterials: Techniques and Applications*; Woodhead Publishing: Cambridge, UK, 2016; pp. 3–33. ISBN 9780081009420.
16. Zhao, C.; Xia, L.; Zhai, D.; Zhang, N.; Liu, J.; Fang, B.; Chang, J.; Lin, K. Designing ordered micropatterned hydroxyapatite bioceramics to promote the growth and osteogenic differentiation of bone marrow stromal cells. *J. Mater. Chem. B* **2015**, *3*, 968–976. [[CrossRef](#)]
17. Lukaszewska-Kuska, M.; Wirstlein, P.; Majchrowski, R.; Dorocka-Bobkowska, B. Osteoblastic cell behaviour on modified titanium surfaces. *Micron* **2018**, *105*, 55–63. [[CrossRef](#)]
18. Palmquist, A.; Lindberg, F.; Emanuelsson, L.; Brånemark, R.; Engqvist, H.; Thomsen, P. Biomechanical, histological, and ultrastructural analyses of laser micro- and nano-structured titanium alloy implants: A study in rabbit. *J. Biomed. Mater. Res. Part A* **2010**, *92*, 1476–1486. [[CrossRef](#)]
19. Agarwal, A.; Schultz, C.; Goel, V.K.; Agarwal, A.; Anand, N.; Garfin, S.R.; Wang, J.C. Implant Prophylaxis: The Next Best Practice Toward Asepsis in Spine Surgery. *Glob. Spine J.* **2018**, *8*, 761–765. [[CrossRef](#)]
20. Subramani, K.; Jung, R.E.; Molenberg, A.; Hammerle, C.H.F. Biofilm on dental implants: A review of the literature. *Int. J. Oral Maxillofac. Implants* **2009**, *24*, 616–626.
21. Liu, M.; Zhou, J.; Yang, Y.; Zheng, M.; Yang, J.; Tan, J. Surface modification of zirconia with polydopamine to enhance fibroblast response and decrease bacterial activity in vitro: A potential technique for soft tissue engineering applications. *Colloids Surf. B Biointerfaces* **2015**, *136*, 74–83. [[CrossRef](#)]
22. Knetsch, M.L.W.; Koole, L.H. New strategies in the development of antimicrobial coatings: The example of increasing usage of silver and silver nanoparticles. *Polymers* **2011**, *3*, 340–366. [[CrossRef](#)]
23. Shah, S.R.; Tatara, A.M.; D'Souza, R.N.; Mikos, A.G.; Kasper, F.K. Evolving strategies for preventing biofilm on implantable materials. *Mater. Today* **2013**, *16*, 177–182. [[CrossRef](#)]
24. Bohinc, K.; Dražič, G.; Fink, R.; Oder, M.; Jevšnik, M.; Nipič, D.; Godič-Torkar, K.; Raspor, P. Available surface dictates microbial adhesion capacity. *Int. J. Adhes.* **2014**, *50*, 265–272. [[CrossRef](#)]
25. Cunha, A.; Elie, A.M.; Plawinski, L.; Serro, A.P.; Botelho Do Rego, A.M.; Almeida, A.; Urdaci, M.C.; Durrieu, M.C.; Vilar, R. Femtosecond laser surface texturing of titanium as a method to reduce the adhesion of *Staphylococcus aureus* and biofilm formation. *Appl. Surf. Sci.* **2016**, *360*, 485–493. [[CrossRef](#)]
26. Alamri, S.; Lasagni, A.F. Development of a general model for direct laser interference patterning of polymers. *Opt. Express* **2017**, *25*, 9603–9616. [[CrossRef](#)]
27. Heiroth, S.; Koch, J.; Lippert, T.; Wokaun, A.; Günther, D.; Garrelie, F.; Guillermin, M. Laser ablation characteristics of yttria-doped zirconia in the nanosecond and femtosecond regimes. *J. Appl. Phys.* **2010**, *107*, 14908. [[CrossRef](#)]
28. Queiroz, A.C.; Santos, J.D.; Vilar, R.; Eugénio, S.; Monteiro, F.J. Laser surface modification of hydroxyapatite and glass-reinforced hydroxyapatite. *Biomaterials* **2004**, *25*, 4607–4614. [[CrossRef](#)]
29. Kurella, A.; Dahotre, N.B. Laser induced hierarchical calcium phosphate structures. *Acta Biomater.* **2006**, *2*, 677–683. [[CrossRef](#)]
30. Triantafyllidis, D.; Li, L.; Stott, F.H. Surface treatment of alumina-based ceramics using combined laser sources. *Appl. Surf. Sci.* **2002**, *186*, 140–144. [[CrossRef](#)]
31. Harimkar, S.P.; Dahotre, N.B. Crystallographic and morphological textures in laser surface modified alumina ceramic. *J. Appl. Phys.* **2006**, *100*, 24901. [[CrossRef](#)]
32. Samant, A.N.; Dahotre, N.B. Laser machining of structural ceramics—A review. *J. Eur. Ceram. Soc.* **2009**, *29*, 969–993. [[CrossRef](#)]
33. Samant, A.N.; Dahotre, N.B. Three-dimensional laser machining of structural ceramics. *J. Manuf. Process.* **2010**, *12*, 1–7. [[CrossRef](#)]
34. Yang, J.; Yu, J.; Cui, Y.; Huang, Y. New laser machining technology of Al₂O₃ ceramic with complex shape. *Ceram. Int.* **2012**, *38*, 3642–3648. [[CrossRef](#)]
35. Li, J.; Ji, L.; Hu, Y.; Bao, Y. Precise micromachining of yttria-tetragonal zirconia polycrystal ceramic using 532 nm nanosecond laser. *Ceram. Int.* **2016**, *42*, 4377–4385. [[CrossRef](#)]

36. Baino, F.; Montealegre, M.A.; Minguella-Canela, J.; Vitale-Brovarone, C. Laser Surface Texturing of Alumina/Zirconia Composite Ceramics for Potential Use in Hip Joint Prosthesis. *Coatings* **2019**, *9*, 369. [[CrossRef](#)]
37. Henriques, B.; Fabris, D.; Souza, J.C.M.; Silva, F.S.; Carvalho, Ó.; Fredel, M.C.; Mesquita-Guimarães, J. Bond strength enhancement of zirconia-porcelain interfaces via Nd: YAG laser surface structuring. *J. Mech. Behav. Biomed. Mater.* **2018**, *81*, 161–167. [[CrossRef](#)]
38. Soon, G.; Pingguan-Murphy, B.; Lai, K.W.; Akbar, S.A. Review of zirconia-based bioceramic: Surface modification and cellular response. *Ceram. Int.* **2016**, *42*, 12543–12555. [[CrossRef](#)]
39. Berger, J.; Roch, T.; Pistillo, N.; Lasagni, A.F. Multiple-beam laser patterning on aluminum oxide, zirconium oxide, and hydroxyapatite ceramic materials using a microlens array. *J. Laser Appl.* **2016**, *28*, 42003. [[CrossRef](#)]
40. Holthaus, M.G.; Treccani, L.; Rezwani, K. Comparison of micropatterning methods for ceramic surfaces. *J. Eur. Ceram. Soc.* **2011**, *31*, 2809–2917. [[CrossRef](#)]
41. Dahotre, N.B.; Harimkar, S.P. *Laser Fabrication and Machining of Materials*, 1st ed.; Springer US: Boston, MA, USA, 2008; ISBN 9780387723433.
42. Roitero, E.; Lasserre, F.; Roa, J.J.; Anglada, M.; Mücklich, F.; Jiménez-Piqué, E. Nanosecond-laser patterning of 3Y-TZP: Damage and microstructural changes. *J. Eur. Ceram. Soc.* **2017**, *37*, 4876–4887. [[CrossRef](#)]
43. Mücklich, F.; Lasagni, A.; Daniel, C. Laser interference metallurgy—Using interference as a tool for micro/nano structuring. *Int. J. Mater. Res.* **2006**, *97*, 1337–1344. [[CrossRef](#)]
44. Lasagni, A.F.; Gachot, C.; Trinh, K.E.; Hans, M.; Rosenkranz, A.; Roch, T.; Eckhardt, S.; Kunze, T.; Bieda, M.; Günther, D.; et al. Direct laser interference patterning, 20 years of development: From the basics to industrial applications. In Proceedings of the Laser-based Micro- and Nanoprocessing XI, San Francisco, CA, USA, 7 March 2017; p. 1009211.
45. Guenther, D.; Valle, J.; Burgui, S.; Gil, C.; Solano, C.; Toledo-Arana, A.; Helbig, R.; Werner, C.; Lasa, I.; Lasagni, A.F. Direct laser interference patterning for decreased bacterial attachment. In Proceedings of the Laser-based Micro- and Nanoprocessing X, San Francisco, CA, USA, 4 March 2016; p. 973611.
46. Valle, J.; Burgui, S.; Langheinrich, D.; Gil, C.; Solano, C.; Toledo-Arana, A.; Helbig, R.; Lasagni, A.; Lasa, I. Evaluation of Surface Microtopography Engineered by Direct Laser Interference for Bacterial Anti-Biofouling. *Macromol. Biosci.* **2015**, *15*, 1060–1069. [[CrossRef](#)] [[PubMed](#)]
47. Langheinrich, D.; Yslas, E.; Broglia, M.; Rivarola, V.; Acevedo, D.; Lasagni, A. Control of cell growth direction by direct fabrication of periodic micro- and submicrometer arrays on polymers. *J. Polym. Sci. Part B Polym. Phys.* **2012**, *50*, 415–422. [[CrossRef](#)]
48. Zwahr, C.; Günther, D.; Brinkmann, T.; Gulow, N.; Oswald, S.; Grosse Holthaus, M.; Lasagni, A.F. Laser Surface Patterning of Titanium for Improving the Biological Performance of Dental Implants. *Adv. Healthc. Mater.* **2017**, *6*, 1600858. [[CrossRef](#)]
49. Daniel, C.; Armstrong, B.L.; Howe, J.Y.; Dahotre, N.B. Controlled evolution of morphology and microstructure in laser interference-structured zirconia. *J. Am. Ceram. Soc.* **2008**, *91*, 2138–2142. [[CrossRef](#)]
50. Daniel, C.; Drummond, J.; Giordano, R.A. Improving flexural strength of dental restorative ceramics using laser interference direct structuring. *J. Am. Ceram. Soc.* **2008**, *91*, 3455–3457. [[CrossRef](#)]
51. Roitero, E.; Lasserre, F.; Anglada, M.; Mücklich, F.; Jiménez-Piqué, E. A parametric study of laser interference surface patterning of dental zirconia: Effects of laser parameters on topography and surface quality. *Dent. Mater.* **2017**, *33*, 28–38. [[CrossRef](#)]
52. Roitero, E.; Ochoa, M.; Anglada, M.; Mücklich, F.; Jiménez-Piqué, E. Low temperature degradation of laser patterned 3Y-TZP: Enhancement of resistance after thermal treatment. *J. Eur. Ceram. Soc.* **2018**, *38*, 1742–1749. [[CrossRef](#)]
53. Berger, J.; Holthaus, M.G.; Pistillo, N.; Roch, T.; Rezwani, K.; Lasagni, A.F. Ultraviolet laser interference patterning of hydroxyapatite surfaces. *Appl. Surf. Sci.* **2011**, *257*, 3081–3087. [[CrossRef](#)]

